Characterization of ALD High-k Dielectrics in GaN and Ga_2O_3 Metal-Oxide-Semiconductor Systems

David I. Shahin[1], Travis J. Anderson[2], Virginia D. Wheeler[2], Marko J. Tadjer[2], Lunet E. Luna[3], Andrew D. Koehler[2], Karl D. Hobart[2], Charles R. Eddy, Jr.[2], Fritz J. Kub[2], and Aris Christou[1]

[1]University of Maryland, College Park, MD 20742, USA, e-mail: dshahin@umd.edu
[2]U.S. Naval Research Laboratory, Washington, DC 20375, USA
[3]NRC Postdoctoral Fellow Residing at NRL

Keywords: ZrO_2, HfO_2, GaN, Ga_2O_3, Dielectric, MOS Capacitor

Abstract

Capacitance-voltage measurements on MOS capacitors have been used to characterize ZrO_2 and HfO_2 dielectrics deposited on bulk GaN and $(\bar{2}01)$ β-Ga_2O_3 by thermal atomic layer deposition. ZrO_2 films were deposited using either zirconium(IV) tert-butoxide (ZTB) or tetrakis(dimethylamido)-zirconium (TDMAZ) and deionized water precursors. HfO_2 was deposited using tetrakis(ethylmethylamino)-hafnium and deionized water precursors. The dielectric constant of ZTB-ZrO_2 films was significantly dependent on frequency between 1 kHz (k~27) and 1 MHz (k~17), likely due to excess oxygen present as defects in the films; TDMAZ-ZrO_2 and HfO_2 exhibited frequency-independent dielectric constants of k~24 and k~14, respectively. ZTB-ZrO_2 films on GaN exhibited positive flatband voltage shifts consistent with negative oxide/interface charge between 5-7x10^{12} cm^{-2}, while TDMAZ-ZrO_2 films exhibited significantly less fixed charge. On β-Ga_2O_3, ZTB-ZrO_2 and HfO_2 exhibited minimal hysteresis, and negative fixed charge on the order of 2x10^{12} cm^{-2}. While an order of magnitude higher interface trap density was estimated for ZTB-ZrO_2 (2x10^{12} $cm^{-2}\cdot eV^{-1}$) compared to HfO_2 (2x10^{11} $cm^{-2}\cdot eV^{-1}$) between 0.2-0.25 eV below the conduction band, both values compare well with other oxides on Ga_2O_3. Further work is needed to understand and mitigate the frequency dependence of ZTB-ZrO_2 while maintaining negative fixed charge.

Introduction

Wide and ultra-wide bandgap semiconductors such as GaN and β-Ga_2O_3 have excellent material characteristics for high-power and high-temperature electronics, including large bandgaps (3.4 and 4.8 eV, respectively) and large predicted critical electric field strengths (3.3 and 8 MV/cm, respectively) [1, 2]. High quality MOS gate structures with these semiconductors are desirable for fail-safe (normally-off) power transistors with low gate leakage.

High-k ALD dielectrics such as ZrO_2 and HfO_2 have become appealing for achieving normally-off behavior in GaN and Ga_2O_3 transistors. The recent demonstration of record positive threshold voltage (V_t) for AlGaN/GaN MOSHEMTs was achieved in part through use of a ZrO_2 gate dielectric deposited by thermal ALD using zirconium (IV) tert-butoxide (ZTB) and deionized water precursors [3]. ZTB-ZrO_2 dielectrics have been the subject of relatively little study in GaN MOS systems compared to ZrO_2 deposited from the more common tetrakis(dimethylamido)-zirconium (TDMAZ) [4]. An HfO_2 dielectric was also recently employed in demonstration of a positive V_t β-Ga_2O_3 MOSFET [5]. ZrO_2 and HfO_2 have recently been demonstrated to have suitable conduction band offsets with β-Ga_2O_3, but to date, only basic electrical characterization has been performed on these high-k oxides on Ga_2O_3 [6]. As such, characterizing and optimizing these dielectrics in GaN and Ga_2O_3 MOS systems is an important undertaking for production of high performance normally-off devices.

Experimental

Simple MOS capacitor structures were used to characterize ALD high-k dielectrics on n-type HVPE GaN (Kyma) and bulk $(\bar{2}01)$ β-Ga_2O_3 (Tamura Corp.), as shown in Fig. 1. Prior to dielectric deposition, GaN samples were cleaned using a variety of surface pretreatments previously found to give high quality interfaces with Al_2O_3 and HfO_2, including piranha ($3H_2SO_4$:$1H_2O_2$) etching at 80 °C followed

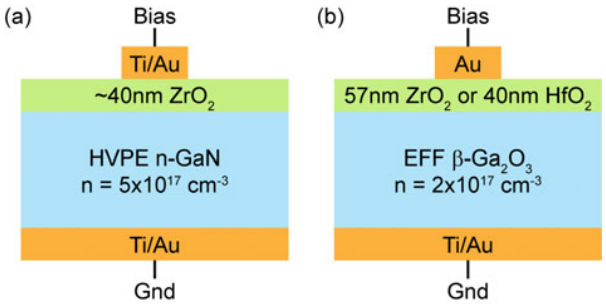

Fig. 1. Cross-sections of MOS capacitors on (a) HVPE-grown GaN films with either 36.8 nm ZTB-ZrO_2 or 39.1 nm TDMAZ-ZrO_2 and (b) EFF-grown β-Ga_2O_3 bulk substrates with either 57 nm ZTB-ZrO_2 or 40 nm HfO_2.

by rapid thermal annealing in flowing O_2 at 700 °C for 10 minutes [7]. Ga_2O_3 bulk substrates were cleaned prior to dielectric deposition with a 10 minute UV/O_3 exposure, followed by a 30 second etch in 10:1 buffered oxide etchant. ZrO_2 or HfO_2 were deposited by thermal ALD after sample cleaning. ZrO_2 films were deposited at 200 °C using either ZTB or TDMAZ and deionized water precursors in an Ultratech Savannah 200 ALD reactor. HfO_2 was deposited at 175 °C in an Oxford FlexAL system using tetrakis(ethylmethylamino)-hafnium and deionized water precursors. MOS capacitors were then fabricated by standard e-beam metal evaporation and liftoff processes according to the structures in Fig. 1. Electrical measurements were performed using a Keithley 4200 semiconductor characterization system. Capacitance-voltage measurements were performed between circular topside contacts on the oxides and large-area backside contacts to the bulk substrates.

Results and Discussion

ZrO_2 on GaN

The frequency response of the ZrO_2 films from each precursor, shown in Fig. 2, was extracted by measuring the capacitance as a function of frequency in accumulation at a fixed bias of +5 V. The ZTB-grown film exhibited a significant frequency dependence of accumulation capacitance and thus dielectric constant (k), with k decreasing from the expected values of ~27 at 1 kHz to ~17 at 1 MHz. The TDMAZ-grown films, however, showed stable capacitance values leading to a dielectric constant of k~24 across the entire measured frequency range. XPS measurements on ZTB films indicated a O:Zr ratio of 2.2:1 [6], while the TDMAZ films were nearly stoichiometric with an O:Zr ratio of 2.0:1. The excess oxygen in the ZTB films is

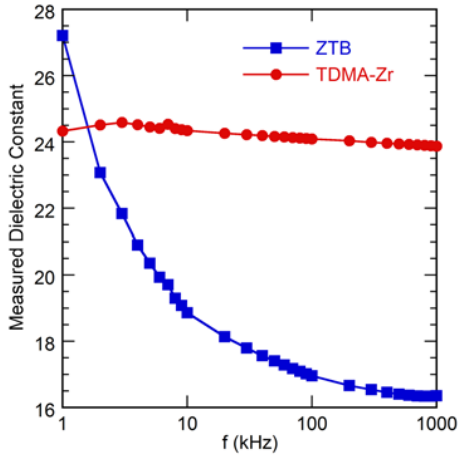

Fig. 2. Extracted frequency-dependent dielectric constants for ZrO_2 films deposited using either ZTB or TDMAZ precursors.

therefore suspected to be the source of the observed frequency dependence, but the exact nature of the excess oxygen (oxygen interstitials, hydroxyl groups, etc.) is still being investigated. Hopefully, this frequency-dependent response can be mitigated through post-deposition annealing or other deposition process modifications, while still preserving the negative fixed charge useful for normally-off power devices.

1 MHz C-V measurements were performed on the ZrO_2/GaN MOS capacitors shown in Fig. 1(a) to compare the effects of the different surface pretreatments (reference acetone and isopropanol rinse, 80 °C piranha clean for 10 minutes, and a piranha clean followed by 700 °C oxygen rapid thermal annealing for 10 minutes) on the C-V characteristics from each precursor. These C-V curves are summarized in Table I and shown graphically in Fig. 3. The measured hysteresis at flatband was much wider ($0.7 \leq \Delta V_{fb} \leq 1.5$ V) than previously observed when employing these surface treatments before deposition of Al_2O_3 and HfO_2 on GaN ($\Delta V_{fb} \leq 0.5$ V) [7]; this may be due to the use bulk HVPE GaN, rather than MOCVD GaN-on-sapphire as in the previous report. Furthermore, for both oxides, the pre-ALD piranha treatment tended to yield the most uniform C-V curves with the lowest hysteresis (and corresponding trapped charge), while the post-piranha thermal oxidation actually worsened the hysteresis.

Table I
Capacitance-Voltage Measurements Comparing ZrO_2 Precursors and Pre-ALD Surface Treatments

ALD Precursor	Surface Treatment	V_{fb} (V)	ΔV_{fb} (V)	Fixed Charge (cm^{-2})	Trapped Charge (cm^{-2})
ZTB	Reference	2.2	1.2	-7.4×10^{12}	4.4×10^{12}
	Piranha	1.9	0.8	-5.4×10^{12}	2.3×10^{12}
	Piranha + Oxidation	2.0	1.0	-5.7×10^{12}	3.1×10^{12}
TDMAZ	Reference	1.8	0.7	-5.0×10^{12}	2.1×10^{12}
	Piranha	0.3	0.8	-4.2×10^{11}	2.6×10^{12}
	Piranha + Oxidation	0.6	1.5	-1.5×10^{12}	5.1×10^{12}

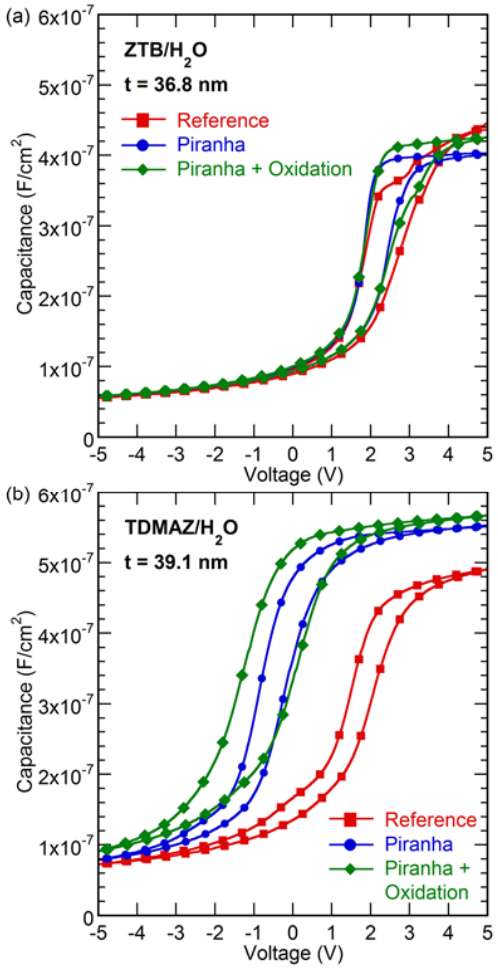

Fig. 3. 1 MHz dual-sweep capacitance-voltage measurements on ZrO_2/GaN MOS-capacitors from (a) ZTB (36.8 nm film thickness) and (b) TDMAZ (39.1 nm film thickness) precursors with various pre-ALD surface treatments.

Compared to the theoretical flatband voltage (V_{fb}) of 0.12 V calculated for these structures, the ZTB-ZrO_2 C-V curves were uniformly shifted to positive voltages, regardless of the pre-ALD surface treatment employed. These shifts are taken to be indicative of an overriding negative fixed charge, again likely excess oxygen, on the order of 5-7x10^{12} cm^{-2}, and is in line with the observed charge densities from ZTB-ZrO_2 MOSHEMTs [3]. Meanwhile, surface treatments before TDMAZ-ZrO_2 deposition produced a negative shift in the measured C-V curves compared to the reference, yielding V_{fb} values much closer to ideal, and a corresponding reduction in fixed charge density to as low as 4x10^{11} cm^{-2}. TDMAZ-ZrO_2 therefore may not be as effective as ZTB-ZrO_2 in producing normally-off behavior in HEMTs and related depletion-mode devices due to the lack of significant negative oxide charge to deplete the device channel.

ZrO_2 and HfO_2 on β-Ga_2O_3

C-V measurements were also performed on ZTB-ZrO_2/Ga_2O_3 and HfO_2/Ga_2O_3 MOS capacitors according to the structure in Fig. 1b. The resulting measured C-V curves, shown in Fig. 4, exhibited less than 0.15 V hysteresis and are comparable to the best reported values for ALD oxide/Ga_2O_3 MOS capacitors [8]. Furthermore, both ZTB-ZrO_2 and HfO_2 exhibited approximately a +1 V positive shift in flatband voltage, relative to the predicted value of 1.1 V calculated from previous studies of Au contacts on Ga_2O_3 [9]. These shifts correspond to a negative oxide fixed charge of 2x10^{12} cm^{-2}, slightly lower than that observed for the high-k oxides on GaN. As shown in Fig. 4a, the ZTB-ZrO_2 again suffers from the same frequency dispersion in accumulation capacitance believed to stem from excess oxygen defects, with the extracted dielectric constant decreasing from k~24 to k~16 between 10 kHz and 1 MHz measurement frequencies. The HfO_2 C-V response (Fig. 4b) was frequency-stable over

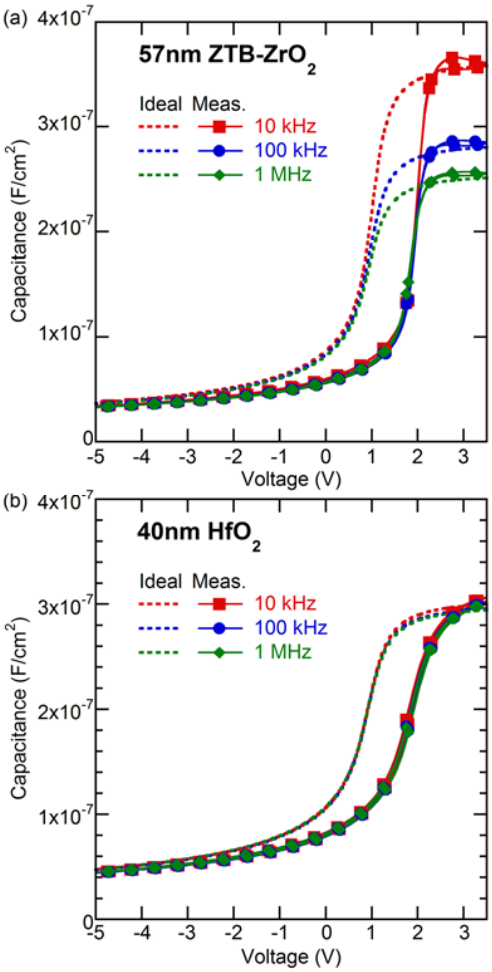

Fig. 4. Ideal and measured (dual-sweep) capacitance-voltage curves for (a) ZTB-ZrO_2/Ga_2O_3 and (b) HfO_2/Ga_2O_3 MOS-capacitors, showing a ~1V positive shift relative to the ideal C-V curves while maintaining extremely low hysteresis.

the same measurement range, with an extracted dielectric constant of k~14.

The ideal C-V curves (dashed lines in Fig. 4) were calculated to allow estimation of interface trap density (D_{it}) through the Terman method using Eqn. 1 [10, 11]:

$$D_{it} = \frac{C_{ox}}{q^2}\left(\frac{dV_g}{d\varphi_s} - 1\right) - \frac{C_s}{q} = \frac{C_{ox}}{q^2}\frac{d\Delta V_g}{d\varphi_s} \quad (1)$$

where C_{ox} = oxide capacitance, V_g = measured gate voltage, C_s = semiconductor capacitance, ΔV_g = difference between measured and ideal gate voltage, and φ_s = surface potential. Comparison of the 1 MHz ideal and real C-V curves indicated average D_{it} values of $2x10^{12}$ $cm^{-2}\cdot eV^{-1}$ and $2x10^{11}$ $cm^{-2}\cdot eV^{-1}$ for ZTB-ZrO_2 and HfO_2, respectively, between 0.2-0.25 eV below the conduction band. The order of magnitude higher D_{it} for ZTB-ZrO_2 is again suspected to be linked to the oxygen excess observed in XPS. Even so, the ZTB-ZrO_2 D_{it} compares relatively well with other oxides such as SiO_2 and Al_2O_3 on β-Ga_2O_3, while the HfO_2/Ga_2O_3 MOS capacitor D_{it} is among the lowest reported to date [8, 12].

CONCLUSIONS

MOS capacitors with ZrO_2 and HfO_2 high-k dielectrics were fabricated on bulk GaN and Ga_2O_3 substrates. On both substrate materials, the dielectric constant of ZrO_2 grown by thermal ALD using ZTB and deionized water was found to decrease significantly when measured at increasing frequencies between 1 kHz (k~27) and 1 MHz (k~17), while ZrO_2 grown using TDMAZ and deionized water exhibited a frequency-independent dielectric constant of k~24. HfO_2 also exhibited a frequency-independent dielectric constant of k~14. Wide hysteresis in these ZrO_2 films on GaN ($0.7\ V \leq \Delta V_{fb} \leq 1.5V$) indicated low 10^{12} cm^{-2} trapped charges in these films. Pre-ALD piranha cleaning typically yielded the lowest hysteresis and smoothest C-V curves. ZTB-ZrO_2 films exhibited positive V_{fb} shifts consistent with negative oxide/interface charge around $5\text{-}7x10^{12}$ cm^{-2}, regardless of what surface treatments were employed, while TDMAZ-ZrO_2 films exhibited V_{fb} much closer to the calculated ideal V_{fb}. ZTB-ZrO_2 and HfO_2 deposited on bulk $(\bar{2}01)$ β-Ga_2O_3, however, exhibited drastically lower hysteresis ($\leq 0.15V$) and minimal stretch-out, indicating a higher quality interface with Ga_2O_3 than with GaN. V_{fb} shifts indicated fixed negative charge of $2x10^{12}$ cm^{-2} for both oxides. Terman method D_{it} values ($2x10^{12}$ $cm^{-2}\cdot eV^{-1}$ and $2x10^{11}$ $cm^{-2}\cdot eV^{-1}$ between 0.2-0.25 eV below the conduction for ZTB-ZrO_2 and HfO_2, respectively) compare well with other reports of lower-k oxides on β-Ga_2O_3. While the ZTB-ZrO_2 and HfO_2 utilized in this study show promise for normally-off devices, further work is needed to mitigate the frequency dependence of ZTB-ZrO_2 while maintaining the negative fixed charge before it can become useful for power devices.

ACKNOWLEDGEMENTS

The authors thank the NRL Institute for Nanoscience (Dean St. Amand, Walter Spratt, Anthony Boyd) for processing equipment and support. This work was supported by the Office of Naval Research partially under Award No. N00014-15-1-2392.

REFERENCES

[1] T.P. Chow, Microelect. Eng. **83**, 112 (2006).
[2] M. Higashiwaki, et al., Appl. Phys. Lett. **100**, 013504 (2012).
[3] T.J. Anderson, et al., Appl. Phys. Expr. **9** [7], 071003 (2016).
[4] K.M. Bothe, et al., IEEE Trans. Elect. Dev. **60** [12], 4119
[5] (2013).
[6] M.J. Tadjer, et al., ECS J. Solid State. Sci. Tech. **5** [9], P468 (2016).
[7] V.D. Wheeler, et al., ECS J. Solid State Sci. Tech. **6** [2], Q3052 (2017).
[8] C.R. English, et al., J. Vac. Sci. Tech. B **32** [3], 03D106 (2014).
[9] H. Zhou, et al., IEEE Elect. Dev. Lett. 37, 1411 (2016).
[10] M. Mohamed, et al., Appl. Phys. Lett. **101**, 132106 (2012).
[11] H.C. Casey, *Devices for Integrated Circuits: Silicon and III-V Compound Semiconductors* (1999).
[12] D.K. Schroder, *Semiconductor Material and Device Characterization* (2006).
[13] K. Zeng, et al., IEEE Elect. Dev. Lett. **37**, 906 (2016).

ACRONYMS

MOS: Metal-Oxide-Semiconductor
ALD: Atomic Layer Deposition
MOSHEMT: MOS-High Electron Mobility Transistor
MOSFET: MOS-Field Effect Transistor
ZTB: Zirconium(IV) Tert-Butoxide
TDMAZ: Tetrakis(dimethylamido)-Zirconium
HVPE: Hydride Vapor Phase Epitaxy
EFF: Edge-Defined Film-Fed
C-V: Capacitance-Voltage
XPS: X-ray Photoelectron Spectroscopy
MOCVD: Metal-Organic Chemical Vapor Deposition